AUGUST 01 2001

# A hybrid BIE/FFP scheme for predicting barrier efficiency outdoors

Shahram Taherzadeh; Kai Ming Li; Keith Attenborough



*J. Acoust. Soc. Am.* 110, 918–924 (2001)
https://doi.org/10.1121/1.1381539



# A hybrid BIE/FFP scheme for predicting barrier efficiency outdoors[a)]

Shahram Taherzadeh[b)]
*Department of Environmental and Mechanical Engineering, The Open University, Walton Hall, Milton Keynes MK7 6AA, United Kingdom*

Kai Ming Li
*Department of Mechanical Engineering, The Hong Kong Polytechnic University, Hung Hom, Kowloon, Hong Kong*

Keith Attenborough
*Department of Engineering, University of Hull, Hull HU6 7RX, United Kingdom*

(Received 16 November 1998; revised 5 August 1999; accepted 2 May 2001)

To assess the acoustical performance of noise screens in the presence of an arbitrary sound speed profile, a numerical scheme based on a combination of the boundary integral and fast field program methods is developed. The Green's function required in the boundary integral is evaluated by a fast field formulation. The procedure is validated by comparing its predictions with other numerical results for simple cases and with measurements for indoor model experiments simulating downward refracting conditions. It is predicted that the performance of a noise screen placed 50 m from the source is reduced considerably by moderate downwind conditions.  [DOI: 10.1121/1.1381539]

PACS numbers: 43.50.Gf, 43.50.Vt, 43.28.Fp [MRS]



## I. INTRODUCTION

Recent years have produced a wealth of models and methods for predicting sound pressure in an outdoor environment. These include both analytical formulas for sound pressure in certain simple cases and numerical methods and algorithms with varying degrees of complexity and efficiency for more complex environments. The analytical models deal mainly with propagation in a homogeneous atmosphere above a plane impedance boundary or one with a simple sound speed gradient.[1] The numerical methods, which handle more general situations, include the fast field program[2–6] (FFP) for a range-independent environment, the parabolic equation method[7] (PE) for a range-dependent atmosphere above a plane boundary, and ray tracing techniques.[8] The first two techniques have found a wide spread use in both underwater and atmospheric acoustics. These numerical models have been able to explain many of the observed influences of atmospheric refraction and turbulence. However, all these methods deal with a plane boundary. If the ground is uneven at a scale that is large compared with the wavelengths of interest, as, for example, in the presence of a sound barrier or a hill, many current FFP and PE methods fail.

There has been a number of theoretical methods to calculate the sound field in presence of a barrier of simple shape by, for example, Pierce[9,10] and Rasmussen.[11] These earlier analyses were based on geometrical ray acoustics. On the other hand, numerical solution of the boundary integral equation [the boundary element method (BEM)] provides a comprehensive and accurate way of accounting for more complex boundaries such as a mixed impedance plane as well as an uneven terrain. This versatile numerical method has been utilized to solve a variety of problems involving nonuniform boundaries.[12–21] All these works have assumed neutral atmospheric conditions and no account has been made of the effects of sound wave refraction due to temperature and/or wind speed variation and turbulence. Moreover, many of these numerical schemes assume an infinitely long line source emitting cylindrical waves impinging on barriers or strips of infinite length parallel to the source.

Li *et al.*[22] have considered diffraction of sound from a bump or a trough with a Gaussian shape. They incorporated sound refraction in the medium by using an expression, originally due to Pekeris,[23] for the sound field in an unbounded medium with a linear sound speed profile. By considering only a rigid boundary or a pressure-release one, they simplified the problem considerably. They used an extension of the method of moments to evaluate the boundary integral (with a Gaussian bump). They reported that a soft ground with a bump or a hard ground with a trough causes a sound field enhancement beyond the shadow zone boundary. The significance of this apparent symmetry was not discussed in their predicted results. Uscinski[24] considered a similar problem above a rigid surface of random roughness. He used an expression derived from the parabolic equation approximation to the wave equation to account for the refraction in the medium. More recently, Salomons[25] has used a parabolic equation approach to study the effect of an absorbing barrier in a refracting medium. His numerical procedure involves starting a one-way parabolic marching solution and terminating the waves that impinge upon the barrier. Consequently, Salomons' method does not include backscattering. West

[a)]Based on a presentation at ICA/ASA '98, June 1998, Seattle.
[b)]Author to whom correspondence should be addressed. Electronic mail: S.Taherzadeh@open.ac.uk

 0001-4966/2001/110(2)/918/7/$18.00 

*et al.*[26] derived the parabolic wave equation with a boundary profile function included. They then proceeded to solve the resulting equation by a "wide angle" PE. The formulation, however, is approximate and valid only for barriers or hills with small slopes. Most of the models discussed here are two-dimensional propagation models (propagation in a plane only) with a few exceptions such as the work of Duhamel.[21] There are few theoretical problems with extending a two-dimensional (2-D) model to a three-dimensional propagation method.[27] But the computational effort is large and would require some approximation. The procedure proposed here is also for two-dimensional propagation model.

Li and Wang[28] have introduced a novel method to simulate the effect of a noise barrier in a refracting atmosphere. In their approach, a conformal mapping technique is used to map the wave equation in a medium where the speed of sound varies exponentially with height above a flat boundary to that for a neutral fluid above a curved surface (a section of a cylinder). Subsequently, they use a BEM program, with a discretization of the resulting curved boundary as well as the barrier, to predict the insertion loss of the barrier. They have validated their method by comparing their predictions with measurements of the insertion loss of a thin barrier in a wind tunnel in downwind and upwind conditions.[29] Their method is restricted to relatively short ranges. Moreover, the requirement for discretizing the whole boundary puts a severe burden on the computation time.

The approach taken in this paper is to account for the refraction of the atmosphere as well as the reflection from the flat impedance boundary in the formulation of the Green's function. This approach is similar to that used by Gerstoft and Schmidt[30] for the evaluation of acoustic and seismic reverberation in an ocean environment.

In the next section, the starting boundary integral equation for our BEM is stated. In the subsequent sections we deal with the discretization of the boundary and the numerical solution of the Green's function. In the final section, some numerical examples are presented and discussed.

## II. THEORY

### A. The boundary integral equation

Assume that a line source produces a time-harmonic sound field in a medium, **D**, bounded by a locally reacting impedance surface, **S**. The surface **S** can have features such as barriers, hills, impedance discontinuities, etc. By means of the Green's theorem, the sound field can be written in an integral form as

$$\varepsilon\phi(\mathbf{r}) = G(\mathbf{r},\mathbf{r}_0) - \int_S \left\{ G(\mathbf{r},\mathbf{r}_s)\frac{\partial\phi(\mathbf{r}_s)}{\partial\mathbf{n}(\mathbf{r}_s)} - \phi(\mathbf{r}_s)\frac{\partial G(\mathbf{r},\mathbf{r}_s)}{\partial\mathbf{n}(\mathbf{r}_s)} \right\} ds, \tag{1}$$

where $G(\mathbf{r},\mathbf{r}_0)$, is the solution of the wave equation in the domain in the absence of scatterers, $\mathbf{r}_s$ is the position vector of the boundary element $ds$, and $\mathbf{n}$ is the unit normal vector out of $ds$. A time convention of $\exp(-i\omega t)$ is assumed. The parameter $\varepsilon$ is dependent on the position of the receiver.[31] It is equal to 1 for $\mathbf{r}$ in the medium, $\frac{1}{2}$ for $\mathbf{r}$ on the flat boundary, and equal to the $\Omega/2\pi$ at edges, where $\Omega$ is the solid angle. The surface **S** contains the flat, locally reacting ground surface and additional features such as a barrier. The contribution to the total field from reflection by the flat ground surface can be taken into account in the Green's function, $G(\mathbf{r},\mathbf{r}_s)$. The surface **S** can be redefined to include the scatterer objects only, excluding the ground surface. The integral is then the contribution of the scattering elements to the total sound field at a receiver position. This integral formulation (first derived by Kirchhoff in 1882) is called the Helmhotz–Kirchhoff wave equation. It is the mathematical formulation of the Huygen's principle. If one allows the receiver points to approach the boundary, one obtains an integral equation for the field potential at the boundary. This boundary integral equation is a Fredholm integral equation of the second kind. Once solved, the contribution of the scatterers can be determined by evaluating the integral in Eq. (1) and calculating the total field for any point in the entire domain, **D**. This is the main boundary integral equation (BIE) for the acoustic field potential in the presence of a nonuniform boundary. The boundary element method (BEM) represents the acoustic propagation in a medium by the boundary integral equation and solves the set of integral equations numerically.

The imposition of a suitable boundary condition is required also. In most cases of interest one can assume a locally reacting impedance boundary condition:

$$\frac{d\varphi}{dn} - ik_0\beta\varphi = 0, \tag{2}$$

where $\beta$, the admittance, can be a function of the position on the boundary. This can be applied to the surface of the plane boundary and to the surfaces of the scatterers. Thus the derivative term of the unknown potential can be written in terms of the potential itself. Hence

$$\varepsilon\phi(r,z) = G(\mathbf{r},\mathbf{r}_0) - \int_S \phi(r_s,z_s)\left\{ ik_0\beta G(\mathbf{r},\mathbf{r}_s) - \frac{\partial G(\mathbf{r},\mathbf{r}_s)}{\partial\mathbf{n}(\mathbf{r}_s)} \right\} ds, \quad \mathbf{r},\mathbf{r}_s \in \mathbf{S}. \tag{3}$$

When discretizing the boundary surface it is assumed that the unknown potential is constant in each element, thereby reducing the integral equation to a set of linear equations.

### B. Method of solving the BIE

The procedure for solving the integral equation (3) adopted here is the one suggested by Mayers[32] and used by Chandler-Wilde[15–17,19] These methods involve using a quadrature technique (Simpsons or Gauss) to discretize the integral and transform it to a set of linear equations. In one dimension it can be described as follows. The integration range is divided into $M$ subdomains or elements, each of length or size $h$. The unknown potential, $\phi$, is assumed to be constant within each element. Then the integral in Eq. (3) becomes

$$\int_S \phi(r_s, z_s)\left\{ ik_0\beta G(\mathbf{r},\mathbf{r}_0) - \frac{\partial G(\mathbf{r},\mathbf{r}_s)}{\partial \mathbf{n}(\mathbf{r}_s)}\right\} ds$$
$$= \sum_{m=1}^{M} \phi(r_m, z_m) \int_{t_m - h/2}^{t_m + h/2} \left\{ ik_0\beta G(\mathbf{r},\mathbf{r}_s) - \frac{\partial G(\mathbf{r},\mathbf{r}_s)}{\partial \mathbf{n}(\mathbf{r}_s)}\right\} ds. \tag{4}$$

In principle, the integral on the right-hand side can be evaluated numerically. Then the BIE [Eq. (4)] becomes

$$\varepsilon \phi(\mathbf{r}) = G(\mathbf{r},\mathbf{r}_0) - \sum_{m=1}^{M} \phi(\mathbf{r}_m)\Lambda(\mathbf{r},\mathbf{r}_m), \tag{5}$$

where $\Lambda(\,)$ denotes the integral on the right-hand side of Eq. (4). Substitution of $\mathbf{r}=\mathbf{r}_n$, $n=1,...,M$, produces a set of $M$ linear equations:

$$\varepsilon \phi(\mathbf{r}_n) + \sum_{m=1}^{M} \phi(\mathbf{r}_m)\Lambda(\mathbf{r}_n,\mathbf{r}_m) = G(\mathbf{r}_n,\mathbf{r}_0), \quad n=1,...,M. \tag{6}$$

The Green's function $G(\mathbf{r},\mathbf{r}_s)$ will be singular at $\mathbf{r}=\mathbf{r}_s$, i.e., at diagonal elements when $n=m$. One can use the principal value of the integral for the integrals involving the singularities (see Ref. 31). Here we state only that the solution of the equation (3) is unique except near characteristic frequencies of the space enclosed by the barrier. The main methods suggested in the literature for overcoming this nonuniqueness problem are the so-called CHIEF method[33–35] and the method of Burton and Miller.[36,37]

## III. THE GREEN'S FUNCTION

In Eq. (3), it remains to evaluate the Green's function and its derivative. The Green's function, $G(\mathbf{r},\mathbf{r}_0)$, represents the sound field in the medium in the absence of the scattering surfaces. In order to minimize the number of elements, the Green's function includes reflection from the flat impedance surface. The procedures for evaluation of this Green's function in different conditions are the concern of the rest of this section.

### A. Neutral medium

As discussed in the Introduction, we consider a two-dimensional problem with an infinitely long line source radiating cylindrical waves in the medium. In this case the boundary integral is a line integral and their numerical evaluation is a relatively simple matter. The corresponding Green's function takes the form[19]

$$G_2(\mathbf{r},\mathbf{r}_0) = -(i/4)\{H_0^{(1)}(k|\mathbf{r}_0-\mathbf{r}|) + H_0^{(1)}(k|\mathbf{r}_0'-\mathbf{r}|)\} + P_\beta(\mathbf{r},\mathbf{r}_0), \tag{7}$$

with

$$P_\beta(\mathbf{r},\mathbf{r}_0) = \frac{i\beta}{2\pi}\int_{-\infty}^{+\infty} \frac{e^{ik[(z+z_0)\sqrt{1-s^2}-(x-x_0)s]}}{\sqrt{1-s^2}(\sqrt{1-s^2}-\beta)} ds, \quad \mathrm{Re}(\beta)>0. \tag{8}$$

In the above expression $H_0^{(1)}(\,)$ is the Hankel function of the first kind, $\mathbf{r}$, $\mathbf{r}_0$, and $\mathbf{r}_0'$ are the receiver, source, and image source positions, respectively. The wavenumber, $k$, and the complex admittance, $\beta$, are dependent on the frequency. The function $P_\beta$ represents the ground wave term. The derivatives of the Green's function in the $x$ and $z$ directions are also given in Ref. 19. When the source and the receiver positions coincide, i.e., when $n=m$, the integral $\Lambda(\,)$ has a removable singularity. The integral can be evaluated analytically by replacing the Hankel functions by their small argument approximations and performing the integration.

Habault[18] uses the alternatives of single and double layer potential expressions to represent the Green's function and its derivative. These are again in terms of Hankel functions.

### B. Evaluation of the Green's function by the FFP method

Since discretization of the boundaries is extremely time consuming, the Green's function must include as many calculations as possible in order to minimize the area of the boundary to be discretized. The Green's function includes the wave field propagating in the domain of the system. As such, it must contain the wave terms reflected from the ground if one is to avoid discretizing the whole ground surface. This device means that it is necessary only to discretize the "scatterer" elements above the ground surface, thus saving on the number of elements and equations to be solved. The method allows for the incorporation of an absorbing ground as well as a rigid one.

The Green's function for a line source radiating cylindrical waves above a locally reacting impedance plane can be written as[38]

$$G(\mathbf{r}_1,\mathbf{r}_2) = \frac{1}{\sqrt{2\pi}}\int_0^\infty \varphi(z_1,z_2,k_r)\exp(ik_rR)\,dk_r, \tag{9}$$

where $\mathbf{r}_2[=(x_2,z_2)]$ and $\mathbf{r}_1[=(x_1,z_1)]$ are the source and receiver position vectors, respectively, and $R[=x_2-x_1]$ is the horizontal separation between them.

In practice, the infinite integral is truncated at a suitable value, say $k_{\max}$, and the integral is replaced by a finite FFT sum. The variable of integration, $k_r$, can be thought of as the horizontal component of the wavenumber. To avoid the possible poles on or near the real $k$ axis, the path of integration is deformed below the real axis,

$$\int_0^\infty = \int_0^{-i\alpha\,\delta k} + \int_{-i\alpha\,\delta k}^{k_{\max}-i\alpha\,\delta k}. \tag{10}$$

This is equivalent to making $k_r$ a complex quantity with the imaginary part relating to an adjustable parameter ($\alpha$). The wavenumber interval, $\delta k$, is given by ($k_{\max}/N_k$) with $N_k$ being the number of integration points.

The kernel function $\varphi$ in Eq. (9) is now independent of range and is in one dimension only. This function is the solution of the one-dimensional Helmholtz equation in the presence of a plane impedance boundary. For a homogeneous fluid this solution is known and is given in terms of direct and reflected plane waves:

$$\varphi=\frac{1}{k_z}\left\{e^{ik_z|z_1-z_2|}+\frac{k_z-k_0\beta}{k_z+k_0\beta}e^{ik_z(z_1+z_2)}\right\}, \qquad (11)$$

with $\beta$ being the specific normalized acoustic admittance of the ground; $k_0$ the wave number $(=\omega/c)$; and $k_z=\sqrt{k_0^2-k_r^2}$.

In an inhomogeneous medium such as a refracting atmosphere or in upwind or downwind conditions with an arbitrary sound speed profile, the potential function cannot be determined analytically. Instead, a scheme similar to the finite element method can be utilized[39,40] whereby the fluid is divided into uniform horizontal layers with the speed of sound and air density assumed to be constant within each layer. The potential in each layer is given by

$$\varphi_i=A_i^{\uparrow}e^{k_{z,i}(z-H_i)}+A_i^{\downarrow}e^{k_{z,i}(H_{i+1}-z)}, \qquad (12)$$

with $A_i$'s being the unknown amplitudes and $H_i$ being the layer altitude. The boundary conditions at the layer boundaries determine the wave potential amplitudes in each layer. These conditions are the continuity of normal particle velocity and the pressure across the boundary. The resulting set of linear equations in unknown amplitudes is set in a global matrix form, $\mathbf{A}\times\mathbf{X}=\mathbf{B}$. Here $\mathbf{X}$ represents the unknown amplitude vector; $\mathbf{A}$, the matrix resulting from the known exponential terms, and $\mathbf{B}$ is the source term.[39,40] This matrix equation is solved to produce the wave amplitudes in all layers. The value of the kernel function at one or more desired positions can then be derived easily. An alternative method is to use a transmission line method to evaluate the transfer function between the source and the receiver layers. This method, however, is less efficient than the global matrix method used in our approach for multiple receiver elevations. The derivative of the Green's function required in the integral $\Lambda$ can also be calculated easily. It has been used to calculate the sound field of an arbitrarily oriented dipole above an interface previously.[41,42] The derivatives of the kernel function in a homogeneous fluid above an absorbing boundary are given by

$$\varphi_x=-i\frac{k_r}{k_z}\left\{e^{ik_z|z_1-z_2|}+\frac{k_z-k_0\beta}{k_z+k_0\beta}e^{ik_z(z_1+z_2)}\right\}, \qquad (13)$$

$$\varphi_z=-i\left\{\text{sign}(z_2-z_1)e^{ik_z|z_1-z_2|}+\frac{k_z-k_0\beta}{k_z+k_0\beta}e^{ik_z(z_1+z_2)}\right\}. \qquad (14)$$

The Green's function in each case is obtained easily by substituting the appropriate kernel function in Eq. (9). The $k_r$ term in the numerator of Eq. (13) comes from differentiation of the exponential function in the Hankel transform [Eq. (9)]. In a layered medium, the boundary conditions are the same as for a monopole source. However, there is a slight difference in the source terms. At the fluid–solid interface where the boundary conditions apply, the source terms for the two derivatives are $e^{ik_z|z_1-z_2|}(k_z-k_0\beta)$ for the $z$ derivative and $k_r e^{ik_z|z_1-z_2|}(1-k_0\beta/k_z)$ for the $x$ derivative. The corresponding term for a monopole is $e^{ik_z|z_1-z_2|}(1-k_0\beta/k_z)$.

A simplifying feature of these calculations is that the Green's function and its two derivatives can be calculated simultaneously because the coefficient matrix is the same for all three and only the forcing term is different.

Once the kernel function is evaluated for all $k_r$, the integral in Eq. (9) can either be evaluated by a quadrature scheme or, since it is a Fourier integral, by the discrete Fourier transform method (DFT). This is the essence of the fast field program for calculating the sound pressure field in an arbitrary, range-independent sound speed profile. In the DFT scheme the integral in Eq. (9) is approximated by two discrete sums:[43]

$$G_m(\mathbf{r})=\frac{i}{4}\frac{\delta k\,N_k^{1/2}}{\pi^{1/2}}\left[e^{2\pi m\alpha/N_k}\sum_{n=1}^{N_k-1}\varphi(z,k_n)e^{-2i\pi mn/N_k}+e^{-2\pi m\alpha/N_k}\sum_{n=1}^{N_k-1}\varphi(z,k_n)e^{2i\pi mn/N_k}\right], \qquad (15)$$

where $G_m(\,)$ refers to the Green's function at the receiver point $\mathbf{r}_m$. One advantage of the FFT method is that the function values at an array of positions with a horizontal grid points $m\ \delta r=2m\pi/k_{\max}\ (m=1\cdots N_k)$ are evaluated at once, thus making possible savings on the number of FFP calculations. The horizontal wave number is given by

$$k_n=(n-i\alpha)\delta k. \qquad (16)$$

Both summations can be performed by a single call to a DFT program. To evaluate the integral correctly, certain modifications are required to the kernel function to account for the truncation of the infinite integral at a finite value and for changing the path of integral away from the real axis to avoid the poles. Without these corrections superficial oscillations, called Gibbs oscillations, are superimposed on the kernel function and have detrimental effects on the accuracy of the final computation of the boundary element matrix. This is overcome in our method by applying a Hanning window to the kernel function.[44] With this windowing, accurate and oscillation-free values of the Fourier transform are obtained and lead to an accurate solution of the BIE.

It should be noted, however, that the Fourier transform is accurate only at distances greater than about two wavelengths. At distances shorter than two wavelengths, the Green's function for the homogeneous case is an accurate approximation since sound speed variations have little effect. This approximation has been implemented in our approach.

## IV. NUMERICAL CONSIDERATIONS

A high level of accuracy is required in evaluating the Green's functions in the boundary integral equation. The FFP values for the pressure are accurate only at the spatial grid points. An interpolation scheme for range points lying between the grid points, while providing accurate values for the magnitude of the pressure, fails to give adequate accuracy for the phase values because of insufficient spatial sampling. In this respect, the midpoint of barrier elements must fall on the grid points of the FFP scheme. Hence, there are constraints on the integration parameters such as truncation value ($k_{\max}$) and the number of integration points ($N_k$). An alternative would be to use the Chirp-Z FFP formulation proposed by Li *et al.*[45] to decouple the wave number and space domain grid

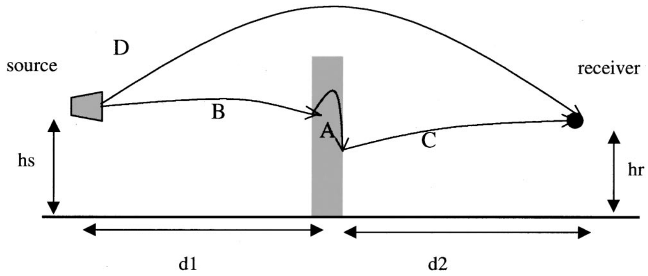


FIG. 1. Schematic diagram to show a typical outdoor environment consisting of a source, receiver, and noise barrier.

values in FFP and have arbitrary grid points in the space domain. However, this approach has not been adopted here.

The three stages to the calculations involving the Green's function and its derivatives are shown in Fig. 1. These stages include the following.

(a) Evaluating the radiation from each element to every other one [i.e., evaluating the matrix elements in Eq. (6)].

(b) Calculating the radiation from the source to each element on the barrier [the right-hand sides of Eq. (6)].

(c) Obtaining the contribution of each barrier element to the sound received at the observation point (i.e., evaluating the boundary integral after the matrix equation has been solved).

In addition, it is necessary to calculate the sound field from the source to the receiver in the absence of the barrier.

While, in principle, a single FFP step is sufficient to evaluate sound pressure at all points in the $x$-$z$ plane, memory considerations make this impractical in most computer systems. Nevertheless, a considerable saving of time can be made at each of the three stages.

Apart from the case where a large area of the boundary has to be discretized (as in an uneven ground surface), the physical size of the scatterer is small compared with the radius of curvature. Furthermore, if the horizontal separation between the elements is small, the sound speed profile plays a very little role. In this case its homogeneous form [Eq. (7)] approximates the Green's function adequately.

The use of FFP in evaluating the Green's function allows one to make efficient computations in certain typical cases. In particular, if the scatterer is a barrier wall with vertical sides, the right-hand sides for each vertical section [case (b) above] can be evaluated with a single FFP step.

The same is true for the third stage (i.e., contributions from each element to a single observer point) by using the reciprocity property of the Green's function and its horizontal (or $x$) derivative.

## V. RESULTS AND DISCUSSION

The numerical program proposed in this paper (BIE-FFP) has been validated by comparing its results to simplified cases where other predictions are available and to attenuation data obtained in laboratory conditions. BIE-FFP predictions for the relatively trivial (albeit computationally intensive, since the entire surface must be discretized) case of a sound field in a refracting medium above a flat absorbing surface, may be compared to theoretical values based on the standard fast field program. The results are shown in Figs. 2 and 3 for upwind and downwind conditions, respectively. In both figures the solid line represents the results of standard FFP calculations of the transmission loss (db *re* field at 1 m) and the circles represent predictions of the BIE-FFP. It is clear that the scheme outlined in this paper is consistent with the standard FFP method for simple cases.

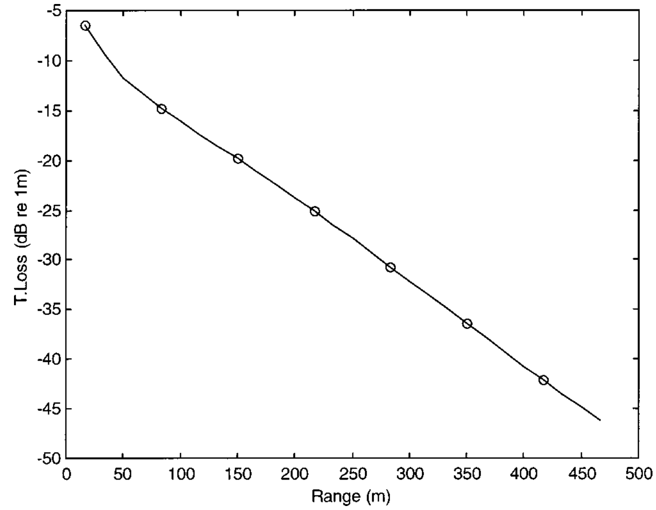


FIG. 2. Sound pressure level in an upwardly refracting medium above an impedance plane as predicted by a FFP code (solid line) and calculated by BIE-FFP and discretizing the boundary to test the code. The source and receiver heights are 10.0 and 1.2 m, respectively. The frequency is 10 Hz and the sound speed gradient is $-1.0\ \mathrm{m}^{-1}$.

Data for the insertion loss of barriers in an arbitrary sound speed profile are rare. Rasmussen[29] has made scale model measurements of the excess attenuation spectra behind a thin barrier in a wind tunnel. The data is taken from Fig. 11 of Ref. 29 and the parameters are (see Ref. 29, Fig. 1): hs=2.0 m, hr=1.0 m, d1=20.0 m, d2=40.0, with the barrier height of 2.5 m. The input wind speed profile is the average of profiles 1 and 2 measured in front and beyond the barrier. Profile No. 3 gave slightly worse predictions. Figure 4 shows the predicted and measured values. There is reasonable agreement between these data (solid line) and the BIE-

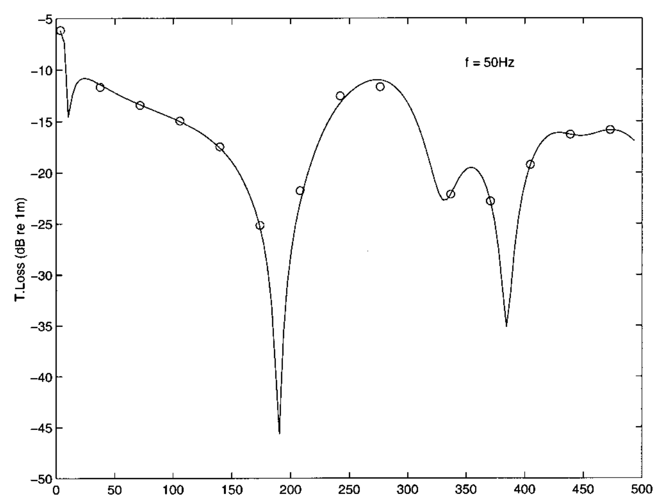


FIG. 3. The same as in Fig. 2, except that the frequency is 50 Hz and the medium is downward refracting. The sound speed gradient is $+1.0\ \mathrm{m}^{-1}$.

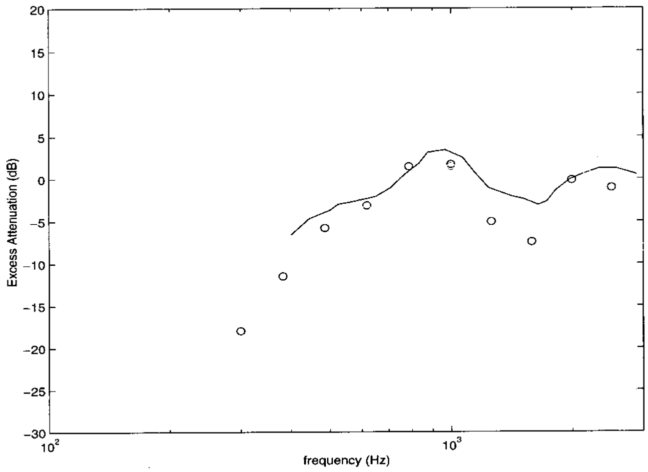


FIG. 4. Measured (solid line: see Fig. 11 of Ref. 24) and predicted (circles) excess attenuation of sound at a receiver behind a barrier 2.5 m high in downwind conditions. The measurement was made in 1:8 scale at a wind tunnel facility. Parameters are hs=2.0 m, hr=1.0 m, d1=20 m, and d2=40 m. A positve sound speed gradient of 0.5 $m^{-1}$ was used.

FFP predictions (circles). These data have been used also by Li and Wang[28] to validate their scheme based on a conformal mapping of a refracting atmosphere to a curved boundary. The BIE-FFP predictions give improved agreement with the measured data.

Another set of measurements have been carried out by Gabillet *et al.*[46] over a hard concave surface with a thin barrier 15 cm high installed on it. The curvature of the surface is analogous to a positive sound speed gradient of 17.0 $m^{-1}$. The source height was 0.1 m, a distance of 4 m away from the barrier. The receiver was 3 m beyond the barrier also at a height of 0.1 m. Figure 5 shows the data [the solid line taken from Fig. 15(c) of Ref. 37] and our prediction (circles) using BIE-FFP. To achieve a stable result, an element size of 1 mm was used in the BIE, and 400 layers were utilized in the FFP

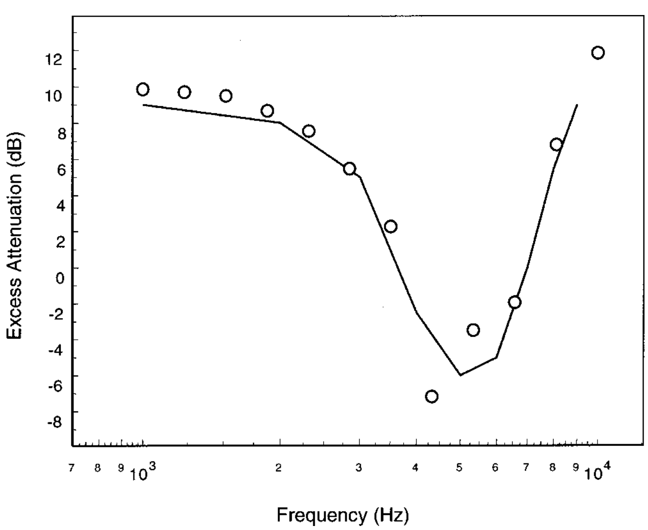


FIG. 5. Measured [solid line: see Fig. 15(c) of Ref. 37] and predicted (circles) excess attenuation of sound behind a thin barrier 0.15 m high on a hard concave surface. Parameters relating to Fig. 1 are hs=0.1 m, hr=0.1 m, d1=4 m, and d2=3 m. The curved surface mapped into a plane boundary resulted in a sound speed gradient of 17 $m^{-1}$.

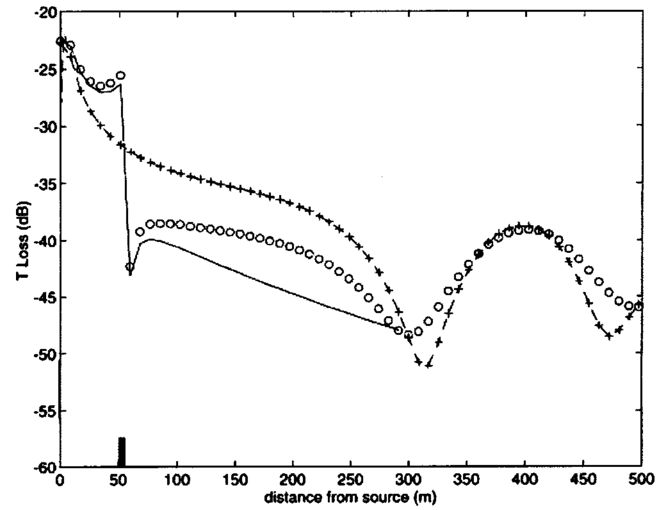


FIG. 6. Effectiveness of a noise barrier under downwind conditions. Crosses: sound level at 500 Hz downwind of the source in the absence of the barrier; Circles: sound level donwwind of the source with a barrier present at a distance of 50 m from the source. Solid line: barrier in the neutral atmosphere. The parameters are hs=0.5 m, hr=1.2 m, $h_{\text{barrier}}$=1.5 m, and a sound speed gradient of +1.0 $m^{-1}$ is assumed. It is seen that after a distance of about 300 m the barrier is no longer effective.

calculations. Again, the BIE-FFP calculations show good agreement with scale model measurements.

We have used the BIE-FFP program to investigate the performance of noise barriers in downwind conditions. We have considered a situation in which an acoustically rigid barrier of height 1.55 m is positioned 50 m downwind of a noise source above an absorbing ground. The transmission loss has been calculated by the BIE-FFP at a frequency of 500 Hz and at observer positions up to a range of 500 m. The predictions of transmission loss with and without the barrier are given in Fig. 6. It is evident that at distances longer than 300 m the barrier is predicted to cause no effective reduction in sound levels. This is consistent with the view that the sound rays effectively curve over the barrier for long distances so that the barrier becomes ineffective.

## VI. CONCLUSION

The model proposed in this paper represents considerable improvement on past applications of the boundary element method to sound propagation above a nonuniform boundary, including the condition of refracting atmosphere, since these have assumed a rigid boundary. We have described a numerical procedure for predicting the sound field in a refracting atmosphere above finite impedance surfaces that include noise barriers and other scatterers. The Green's functions required by the BIE are calculated by the FFP method.

The BIE-FFP has been validated by comparison with widely accepted results for simplified cases and with laboratory measurements reported by other workers.

## ACKNOWLEDGMENT

This work was supported by the EPSRC (UK) Grant No. GR/L15326.

[1] K. M. Li, ‘‘On the validity of the heuristic ray-trace-based modification to the Weyl Van der Pol formula,’’ J. Acoust. Soc. Am. **93**, 1727–1735 (1993).
[2] F. R. DiNapoli, ‘‘A fast field program for multilayered media,’’ Naval Underwater Systems Center, Tech. Rep. 4103, 1971.
[3] R. Raspet, S. W. Lee, E. Kuester, D. C. Chang, W. F. Richards, R. Gilbert, and N. Bong, ‘‘Fast field program for a layered medium bounded by complex impedance surfaces,’’ J. Acoust. Soc. Am. **77**, 345–352 (1985).
[4] S. W. Lee, N. Bong, W. F. Richards, and R. Raspet, ‘‘Impedance formulation of the fast field program for acoustic wave propagation in the atmosphere,’’ J. Acoust. Soc. Am. **79**, 628–634 (1986).
[5] S. J. Franke and G. W. Swenson, Jr., ‘‘A brief tutorial on the fast field program applied to sound propagation in the air,’’ Appl. Acoust. **27**, 203–216 (1989).
[6] S. Tooms, S. Taherzadeh, and K. Attenborough, ‘‘Sound propagation in a refracting fluid above a fluid-saturated porous elastic material,’’ J. Acoust. Soc. Am. **93**, 173–181 (1993).
[7] M. J. White and K. E. Gilbert, ‘‘Application of the parabolic equation to the outdoor propagation of sound,’’ Appl. Acoust. **27**, 227–238 (1989).
[8] K. M. Li, S. Taherzadeh, and K. Attenborough, ‘‘An improved ray-tracing algorithm for predicting sound propagation outdoors,’’ J. Acoust. Soc. Am. **104**, 2077–2083 (1998).
[9] A. D. Pierce, ‘‘Diffraction of sound around corners and over wide barriers,’’ J. Acoust. Soc. Am. **55**, 941–955 (1974).
[10] A. D. Pierce, *Acoustics, An Introduction to its Physical Principles and Applications* (McGraw-Hill, New York, 1980).
[11] K. B. Rasmussen, ‘‘On the effect of terrain profile on sound propagation outdoors,’’ J. Sound Vib. **98**, 35–44 (1985).
[12] M. E. Friedman and R. P. Shaw, ‘‘Diffraction of a plane shock wave by an arbitrary rigid cylindrical obstacle,’’ J. Appl. Mech. **29**, 40–49 (1962).
[13] R. P. Shaw and M. E. Friedman, ‘‘Diffraction of a plane shock wave by a free cylindrical obstacle at a free surface,’’ 4th US National Congress of Applied Mechanics, 1962, pp. 371–379.
[14] R. Seznec, ‘‘Diffraction of sound around barriers: use of the boundary elements technique,’’ J. Sound Vib. **73**, 195–209 (1980).
[15] S. N. Chandler-Wilde and D. C. Hothersall, ‘‘Sound above an inhomogeneous impedance plane,’’ J. Sound Vib. **98**, 475–491 (1985).
[16] S. N. Chandler-Wilde and D. C. Hothersall, ‘‘Propagation of road traffic noise over ground of mixed type,’’ in *Preceedings of the Institute of Acoustics, 1985*, Vol. 7, pp. 367–374.
[17] S. N. Chandler-Wilde, ‘‘Ground effects in environmental sound propagation,’’ Ph.D. thesis, University of Bradford, 1988.
[18] D. Habault, ‘‘Sound propagation above an inhomogeneous plane,’’ J. Sound Vib. **100**, 55–67 (1985).
[19] D. C. Hothersall, S. N. Chandler-Wilde, and M. N. Hajmirzae, ‘‘Efficiency of single noise barriers,’’ J. Sound Vib. **146**, 303–322 (1991).
[20] K. Attenborough, P. Boulange, S. Taherzadeh, and K. M. Li, ‘‘Rough hard surface ground effects,’’ Inter-Noise97, Hungary, 1977.
[21] E. Duhamel, ‘‘Efficient calculation of the three-dimensional sound pressure field around a noise barrier,’’ J. Sound Vib. **197**, 547–571 (1996).
[22] Y. L. Li, S. J. Franke, and C. H. Liu, ‘‘Wave scattering from a ground with a Gaussian bump or trough in an inhomogeneous medium,’’ J. Acoust. Soc. Am. **94**, 1067–1675 (1993).
[23] C. L. Pekeris, ‘‘Theory of propagation of sound in a half-space of variable sound velocity under conditions of formation of a shadow zone,’’ J. Acoust. Soc. Am. **18**, 295–315 (1946).
[24] B. J. Uscinksi, ‘‘Sound propagation with a linear sound-speed profile over a rough surface,’’ J. Acoust. Soc. Am. **94**, 491–498 (1993).
[25] E. M. Salomons, ‘‘Diffraction by a screen in a downwind sound propagation: A parabolic-equation approach,’’ J. Acoust. Soc. Am. **95**, 3109–3117 (1994).
[26] M. West and R. A. Sack, ‘‘A new generalized terrain parabolic equation (GT-PE),’’ in *Proceedings of the 6th International Symposium on Long-Range Sound Propagation*, held in Ottawa, Canada, 1994, pp. 385–391.
[27] L. A. de Lacerda, L. A. Wrobel, H. Power, and W. J. Mansur, ‘‘A novel boundary integral formulation for three-dimensional analysis of thin barriers over an impedance plane,’’ J. Acoust. Soc. Am. **104**, 671–678 (1998).
[28] K. M. Li and Q. Wang, ‘‘A BEM approach to assess the acoustic performance of noise barriers in the refracting atmosphere,’’ J. Sound Vib. **211**, 663–681 (1998).
[29] K. B. Rasmussen, ‘‘Sound propagation over screened ground under upwind conditions,’’ J. Acoust. Soc. Am. **100**, 3581–3586 (1996).
[30] P. Gerstoft and H. Schmidt, ‘‘A boundary element approach to ocean seismoacoustic facet reverberation,’’ J. Acoust. Soc. Am. **89**, 1629–1642 (1991).
[31] R. P. Shaw, ‘‘Boundary integral equation methods applied to wave problems,’’ in *Developments in Boundary Element Methods—1*, edited by P. K. Banerjee and R. Field (Applied Science Publishers, London, 1980).
[32] D. F. Mayers, ‘‘Quadrature methods for Fredholm equations of the second kind,’’ in *Numerical Solution of Integral Equations*, edited by L. M. Delves and L. Walsh (Clarendon, Oxford, 1974).
[33] H. A. Schenck, ‘‘Improved integral formulation for acoustic radiation problems,’’ J. Acoust. Soc. Am. **44**, 41–58 (1968).
[34] A. F. Seybert and T. F. Rengarajan, ‘‘The use of CHIEF to obtain unique solution for acoustic radiation using boundary integral equations,’’ J. Acoust. Soc. Am. **81**, 1299–1306 (1987).
[35] T. W. Wu and A. F. Seybert, ‘‘A weighted residual formulation for the CHIEF methods in acoustics,’’ J. Acoust. Soc. Am. **90**, 1608–1914 (1996).
[36] W. S. Hwang, ‘‘A boundary integral method for acoustic radiation and scattering,’’ J. Acoust. Soc. Am. **101**, 3330–3335 (1997).
[37] A. J. Burton and G. F. Miller, ‘‘The application of integral equation methods to the solution of some exterior boundary-value problems,’’ Proc. R. Soc. London, Ser. A **323**, 201–210 (1971).
[38] P. M. Morse and K. U. Ingard, *Theoretical Acoustics* (McGraw-Hill, New York, 1968), Chap. 7.
[39] K. Attenborough, S. Taherzadeh *et al.*, ‘‘Benchmark cases for outdoor sound propagation models,’’ J. Acoust. Soc. Am. **97**, 173–191 (1995).
[40] F. B. Jensen, W. A. Kuperman, M. B. Porter, and H. Schmidt, *Computational Ocean Acoustics* (American Institute of Physics, Woodbury, NY, 1994), Appendix A4.
[41] S. Taherzadeh and K. Attenborough, ‘‘Sound propagation from dipole and monopole sources in a stratified fluid above a layered poro-elastic solid,’’ in *Proceedings of the Symposium on Computational Acoustics*, edited by C. A. Brebia (Southampton, UK, 1995), pp. 45–54.
[42] S. Taherzadeh, ‘‘Sound propagation in inhomogeneous media,’’ Ph.D. thesis, The Open University, 1996.
[43] T. L. Richards and K. Attenborough, ‘‘Accurate FFT-based Hankel transforms for predictions of outdoor sound propagation,’’ J. Sound Vib. **109**, 157–167 (1986).
[44] D. K. Wilson, ‘‘Use of wavenumber-domain windows in fast field programs,’’ J. Acoust. Soc. Am. **89**, 448–450 (1991).
[45] Y. L. Li, S. J. Franke, and C. H. Liu, ‘‘Numerical implementation of an adaptive fast-field program for sound propagation in layered media using the chirp z transform,’’ J. Acoust. Soc. Am. **89**, 2068–2075 (1991).
[46] Y. Gabillet, H. Schroeder, G. A. Daigle, and A. L'Esperance,, ‘‘Application of the Gaussian beam approach to sound propagation in the atmosphere: Theory and experiments,’’ J. Acoust. Soc. Am. **93**, 3105–3116 (1993).